Large scale networks for human hand-object interaction: Functionally distinct roles for two premotor regions identified intraoperatively

Luciano Simone [a,*], Luca Fornia [a], Luca Viganò [b], Fabio Sambataro [c], Marco Rossi [b], Antonella Leonetti [b], Guglielmo Puglisi [a], Henrietta Howells [a], Andrea Bellacicca [a], Lorenzo Bello [b], Gabriella Cerri [a]

[a] Laboratory of Motor Control, Department of Medical Biotechnologies and Translational Medicine, Università degli Studi di Milano, Humanitas Reasearch Hospital, IRCCS, Milan, Italy
[b] Unit of Neurosurgical Oncology, Department of Oncology and Hemato-Oncology, Università degli Studi di Milano, Humanitas Reasearch Hospital, IRCCS, Milan, Italy
[c] Department of Neuroscience (DNS), University of Padova, Padua, Italy

ARTICLE INFO

The development of awake intraoperative brain-mapping procedures for resection of brain tumors is of growing interest in neuroscience, because it enables direct testing of brain tissue, previously only possible in non-human primates. In a recent study performed in this setting specific effects can be induced by direct electrical stimulation on different sectors of premotor cortex during the execution of a hand manipulation task. Specifically, direct electrical stimulation applied on a dorsal sector of precentral cortex led to an increase in motor unit recruitment in hand muscles during execution of a hand manipulation task (Recruitment sector). The opposite effect was elicited when electrical stimulation was delivered more ventrally on the precentral cortex (Suppression sector). We studied whether the different effects on motor behavior induced by direct electrical stimulation applied on the two sites of the precentral cortex underlie differences in their functional connectivity with other brain areas, measured using resting state fMRI. Using healthy adults scanned as part of the Human Connectome Project, we computed the functional connectivity of each sector used as seeds. The functional connectivity patterns of the two intraoperative seeds was similar but cross-comparison revealed that the left and right Recruitment sectors had stronger functional connections with the hand region of the sensorimotor cortex, while the right Suppression region displayed stronger functional connectivity with a bilateral set of parieto-frontal areas crucial for the integration of perceptual and cognitive hand-related sensorimotor processes required for goal-related hand actions. Our results suggest that analyzing data obtained in the intraoperative setting with resting state functional magnetic resonance imaging in healthy brains can yield useful insight into the roles of different premotor sectors directly involved in hand-object interaction.

1. Introduction

Understanding the neural mechanisms underlying the execution of hand-object interaction is a key issue in systems neuroscience. The undisputed role of premotor cortex in control of highly skilled hand movements has been suggested to be mediated by a ventral sector (PMv) and a dorsal sector (PMd) jointly involved in controlling different aspects of hand-object interactions (see, Dum and Strick, 2005; Borra et al., 2017).

In humans, functional magnetic resonance imaging (fMRI) (e.g Binkofski et al., 1999; Ehrsson et al., 2000; Culham et al., 2003) and transcranial magnetic stimulation (TMS)-induced virtual lesions (Davare et al., 2006, 2008, 2009) studies show the involvement of both PMv and PMd in the execution of reach-to-grasp actions. However, indirect measurements of brain activity provided by fMRI and the poor spatial resolution of TMS prevents clear attribution of the effect of TMS to a specific cortical sector, thus it is can be challenging to infer the role of different sectors in control of the hand.

In a recent study performed in the neurosurgical setting, somatotopy and excitability of the PMv region was mapped with high spatial resolution using direct electrical stimulation (DES), delivered in awake patients undergoing intraoperative brain mapping during neurosurgical procedures for resection of brain tumors (Fornia et al., 2018). In the same clinical setting, quantitative analysis of the causal effect of DES on the electromyographic activity (EMG) of hand muscles engaged in the execution of a hand manipulation task was performed. Precisely, changes in recruitment of motor units of hand muscles active during the execution of the task were investigated. Results showed that DES clearly disrupted task execution with different features when delivered in different sectors of the precentral gyrus: when DES was applied on the dorsal sector, a dysfunctional increase in motor unit recruitment was reported (we term this the "Recruitment" sector), as quantified by the Root Mean Square (RMS) measured on the EMG of hand muscles. The RMS from each muscle was used to quantify the amount of motor units recruited by the task execution. Conversely, DES delivered on the more ventral sector resulted in a decrease in motor unit recruitment (we term the "Suppression" sector). These results point to a differential role of the two premotor subsectors in shaping motor output during hand manipulation task (Fornia et al., 2019). It is likely the functional differences of these two sectors are subserved by different cortical and subcortical connectivity, however this has not yet been studied.

The functional connectivity of these two premotor sectors can be probed using resting-state fMRI (rsfMRI), a relatively recent imaging technique that evaluates the synchrony of low frequency fluctuations of Blood Oxygen Level Dependent (BOLD) contrast at rest in the entire brain. Although the exact matching between functional and anatomical connectivity remains to be fully demonstrated, there is general consensus that they are associated (Honey et al., 2009; Deco and Corbetta, 2011; Behrens and Sporns, 2012; Wang et al., 2013). Interestingly, the networks revealed at rest by rsfMRI often overlap with networks revealed by task-based functional MRI during performance of motor and cognitive tasks (Biswal et al., 1995; Power et al., 2011). Moreover, the functional networks highlighted by rsfMRI are evaluated when measuring the effect of neuroplasticity on motor pathways associated with motor learning or to recovery of function following brain lesions (Guerra-Carrillo et al., 2014; Baldassarre et al., 2016).

Recent papers have shown that an analysis of the effect of DES in the intraoperative setting combined with rsfMRI provides useful information to disclose the role of regions stimulated with DES and to identify the brain networks in which they are embedded (Zacà et al., 2018; Yordanova et al., 2018; Viganò et al., 2019). Based on these premises, we here aimed to disclose the functional networks of two premotor sectors involved in highly skilled hand movement, i.e. hand-object interaction. We employed a multimodal approach by combining the results obtained with DES in the intraoperative setting with functional connectivity estimated with rsfMRI. Specifically, we computed the functional connectivity of premotor cortical subsectors identified with DES (Recruitment and Suppression sectors according to Fornia et al., 2019) to identify their functional networks. As two subsectors were characterized based on quantitative analysis of hand muscles, the anatomical coordinates were thus functionally derived, corresponding with specific features of the skilled hand task performed intraoperatively. Furthermore, within each hemisphere, seeds were defined within a large cohort of patients and, to compensate for sparse sampling, anatomical clustering of the seeds were estimated by means of a probability density function. Finally, functional connectivity of the seeds identified by DES were computed using a population of healthy subjects from the Human Connectome Project (Van Essen et al., 2013). This was crucial to avoid possible artefacts or bias due to the presence of glial tumors, reported to reduce ipsilesional BOLD activity (Schreiber et al., 2000). We evaluated the likely white matter tracts that may support our functional findings, using Tractotron software (Rojkova et al., 2016).

2. Material and methods

2.1. Patient selection

Sixty-six right-handed neurosurgical patients who underwent an asleep-awake-asleep procedure with the aid of the brain mapping technique for removal of a tumor located in the right (n = 30) or left (n = 36) hemisphere were included in our study. Their ages ranged from 15 to 65 years. Preoperatively, all patients were assessed using a neurological and neuropsychological evaluation of cognitive abilities (language, memory, executive function and attention, for a comprehensive description of the neuropsychological battery see Rossi et al., 2018) including upper limb apraxia (ideomotor-apraxia test, Spinnler and Tognoni, 1987). The scores obtained by patients considered for the study fell within the normal range. Inclusion criteria for patients was that the tumor was not infiltrating the investigated areas. Patients who received previous neurosurgical treatment were not included. Only patients without seizures, or at least, with a short seizure history well-controlled with only one anti-epileptic drug, were included. All patients gave written informed consent to the surgical and mapping procedure, which followed the principles outlined in the "World Medical Association Declaration of Helsinki of 1975, as revised in 2008: Research involving human subjects". The study was performed with strict adherence to the routine procedure normally utilized for surgical tumor removal. Accordingly, all data analysed was recorded during the electrophysiological monitoring and stimulating protocols (see below) adopted for routine clinical mapping. The resection was performed in all patients according to functional borders identified by Direct Electrical Stimulation (DES).

2.2. Intraoperative mapping and task description

All patients underwent the standard brain mapping used to preserve language, motor (Bello et al., 2014) and executive function (Puglisi et al., 2018, 2019). To avoid post-operative praxis deficits, all patients performed a hand manipulation task to fulfil clinical purposes, i.e. a task requiring hand-object interaction (for further details see Rossi et al., 2018; Fornia et al., 2019). Specifically, brain mapping was performed by delivering LF-DES (60 Hz) at cortical and subcortical sites of precentral gyrus during hand manipulation task execution to identify and preserve, by monitoring the effect of DES on task execution, sites identified as "positive/effective". A specific tool was made for this purpose. It consists of a small cylindrical handle (⌀ 2 and length 6 cm) inserted inside a fixed rectangular base (3 × 3 cm and 9 cm of length) by means of a worm-screw. The rectangular base was kept stable close to the patient's hand along the armrest of the operating table, while the patient sequentially grasped, hold, rotated and released the cylindrical handle continuously with the thumb and the index finger, using a precision grip. The proximity between the hand and the cylindrical handle allowed the patients to perform the movement using just the fingers, avoiding any reaching movements. Each patient, opportunely trained the day before surgery, was asked to repeat the task with the highest regularity paced by an internal generated rhythm, without any external cue or visual information about the hand or the cylindrical handle movement, thus relying muscle control during hand-object manipulation only on tactile and proprioceptive feedback. During the procedure a trained neuropsychologist performed real-time monitoring of the patients' hand manipulation task behavioral outcome, reporting real time to the surgeons any behavioral impairment in task performance and/or any somatic sensation reported by the patient. Moreover, any impairment was monitored online by the occurrence of a clear anomalous pattern of activation in hand-forearm muscles recorded by EMG.

2.3. Topography of tumor location

Preoperative MRI was performed in all patients on a Philips Intera 3 T scanner (Best). For each patient, the glioma was first segmented into

native space and the T1 volume and segmented tumor were normalized to the Montreal Neurological Institute brain template using the Clinical Toolbox in SPM (ref). Finally, all lesions were superimposed on a template brain using MRICron to create a lesion overlap map.

2.4. Stimulation parameters

DES during the execution of the hand manipulation task was delivered at the Low Frequency (LF-DES). It consisted of trains, lasting 2–5 s, of biphasic square wave pulses (0.5 ms each phase) at 60 Hz (ISI 16.6 ms) delivered by a constant current stimulator (OSIRIS-NeuroStimulator, Inomed) integrated into the ISIS-System through a bipolar probe (2 ball tips, 2 mm diameter, separation 5 mm). The average current released was 3.14 ± 0.75 mA for the left hemisphere and 3.02 mA ± 0.75 mA for the right hemisphere.

2.5. Quantitative EMG analysis of hand muscles: characterization of two effects of DES

In this section we provide a brief description of the methodological procedures, extensively explained in Fornia et al., 2019, adopted to quantify the effect of DES on muscle unit recruitment. Correct and stable hand manipulation task execution, recorded before stimulation, was characterized by a rhythmic EMG pattern of the recorded muscles (Extensor Digitorum Communis, First Dorsal Interosseous and Abductor Pollicis Brevis). Depending on the effect of DES on hand manipulation task execution, cortical sites were classified as *effective*, i.e. DES disrupted task execution, or *ineffective*, where DES did not affect execution. Two quantitative parameters were calculated on the EMG in each muscle across the different conditions (Effective and Ineffective) and the baseline, muscle activity recorded during the task execution in absence of stimulation, in order to quantify the EMG pattern of interference during hand manipulation task:

- The **Autocorrelation coefficient** (aCC), was computed, in each patient, on all the EMG time window selected (i.e. Baseline and DES-related) for each muscle. The aCC analysis (Matlab function "xcorr", using the "unbiased" option) was applied on each EMG window selected, after being demeaned, full-wave rectified and low-pass-filtered; the resulting autocorrelation function, when a phasic activity was maintained, was characterized by a prominent positive peak whose timing corresponded to the fundamental time period (f0), inverse of the fundamental frequency; the y-value of this peak was the aCC index accounting for the regularity/rhythmicity of the phasic muscle contraction during task execution. The closer to the unitary value the peak aCC index is, the more repeatable and regular is to be considered the EMG pattern. The aCC for each muscle strictly reflected the regularity of the EMG pattern and thus the degree of patient performance. This analysis was chosen to provide a quantitative estimation of the effect of DES on hand manipulation task execution.
- The **Root Mean Square** (RMS) was estimated on the same EMG time window selected for the aCC analysis. The RMS of each muscle during effective and ineffective stimulations was normalized to the RMS activity of the corresponding muscle recorded at baseline (see Fornia et al., 2019). We used the normalized RMS from each muscle to quantify the amount of motor units recruited during task execution. These parameters allowed for estimation of the effect of DES on motor unit recruitment in all muscles, irrespective of the rhythmicity of hand manipulation task execution, to disclose whether the effect of DES was mainly excitatory or inhibitory.

Based on aCC and RMS parameters we showed that LF-DES delivery over the effective sites evoked different degrees of muscle impairment during hand manipulation task execution. Stimulation of the dorsal sector of ventral premotor cortex evoked a wide range of complete (arrest pattern) to partial (clumsy pattern) muscle impairment. The RMS

analysis showed that these effects were mainly due to general muscle suppression (motor unit suppression sectors, Supplementary Video 1). Differently, stimulation of the most dorsal investigated sector in PMd also evoked a complete arrest of the task (aCC arrest pattern), however characterized by a general muscle recruitment preceded by brief muscle suppression lasting on average about 320 ms (motor unit recruitment sectors, Supplementary Video 2). These effects occurred in both hemispheres of the right-handed patients selected. Furthermore, to test the occurrence of DES-related motor unit recruitment even in absence of the background voluntary muscle activity (increasing the excitability of the motoneuronal pools) due to the hand manipulation task execution, the effective sites were stimulated with the hand at rest, which failed to elicit clear overt muscle activity. Significant variation in muscle recruitment was estimated using the average $\pm$ 2SD of RMS activity during baseline execution. Notably. this result therefore suggests that these responses, despite evoked in sites very close to the anatomically defined M1-upper limb representation, are not directly mediated by M1 cortico-spinal projections. Stimulation of more caudal sectors close to the central sulcus evoke clear and progressive muscle recruitment both in terms of magnitude and number of muscles involved, depending on the intensity of the current and stimulation time (Fornia et al., 2019). Moreover, stimulation of these sites during tonic closure of the hand evokes slight and slow progressive decrease of EMG activity, which is completely different from the abrupt response obtained during hand manipulation task execution. Results highlight the fact that the regions investigated in the present paper through rsfMRI are functionally distinct sectors possibly involved in different aspects of hand-object interaction. This conclusion is also supported by the presence of a sector of precentral cortex between the two functional sectors, at which DES did not significantly affect muscle activity during hand manipulation task execution. This supports the concept that DES has high spatial resolution and specificity when coupled with an appropriate task.

Supplementary video related to this article can be found at https://doi.org/10.1016/j.neuroimage.2019.116215.

2.6. Definition of seed regions of interest

Each effective stimulation site was used to calculate a three-dimensional visualisation of the most probable region where task performance disruption was likely to occur, based on the concentration of stimulation sites. We performed a probability density function (PDF) based on kernel density estimation (see Supplementary Fig. 2). This was estimated using an in-house script employing non-parametric kernel density estimation from the Statistics toolbox in Matlab (ksdensity function) that works only for 1D and 2D distribution points. First, a 2D PDF was obtained for every cartesian planes zeroing the x, y, and z coordinate of every points and estimating the 2D PDF on a case-by-case basis. Then, each 2D PDF was extended in a 3D volume resembling the volume occupied by all the stimulation sites. The extension was performed copying the 2D PDF in every plane parallel to the PDF and enclosed by the 3D volume. Eventually, the three volumes obtained were multiplied to reconstruct a 3D representation of the probability density function (see Supplementary Fig. 2 and for further details see Fornia et al., 2019).

2.7. Resting state MRI acquisition and sample group

Functional connectivity of minimally preprocessed rsfMRI data of 32 healthy unrelated adults (age: 22–35, 14 males) from the Human Connectome Project (HCP) S1200 release of resting state fMRI (Van Essen et al., 2013) were used for this study. Data included 1200 frames of multiband, gradient-echo planar imaging (Smith et al., 2013) acquired in approximately 15 min with the following parameters: echo time, 33.1 ms; flip angle, 52°; field of view, 280×180 mm; matrix, 140×90; and voxel dimensions, 2 mm isotropic resolution; TR, 0.72 s (Ugurbil et al., 2013). In this study we analysed only one of the four runs acquired

for each subject (left-right encoded). In order to exclude that the phase encoding direction affect the results, in half of subjects seed-based correlation was computed analysing the run acquired with reversed phase encoding.

2.8. rsfMRI data analysis

The low-frequency spontaneous fluctuations in BOLD signal of Recruitment and Suppression seeds identified by DES were cross-correlated voxelwise with every other signal time-course in a whole brain analysis. This produced whole-brain functional connectivity maps representing the strength of correlated resting state signal fluctuations for each seed volume.

Seeds-based correlational analyses were conducted using the Functional Connectivity (CONN) toolbox (http://www.nitrc.org/projects/conn), a Matlab/SPM-based cross-platform open-source software. The minimal preprocessing pipeline for functional MRI, developed by the HCP, was applied to achieve spatial artefact/distortion removal, cross-modal registration, and alignment to standard space (Glasser et al., 2013). Image pre-processing methods were conducted using the Statistical Parametric Mapping 12 (SPM12) software (http://www.fil.ion.ucl.ac.uk/spm/). Briefly, images were corrected for slice time and motion, co-registered with a high-resolution anatomical scan, normalized into the Montreal Neurological Institute space, resampled at $2\,mm^3$, and smoothed with a Gaussian kernel of $6\,mm^3$ full-width half-maximum (Friston et al., 1995). After pre-processing, images were band-pass filtered to $0.008\,Hz–0.09\,Hz$ and motion regressed to diminish the impact of noise.

1st level analysis. The CONN toolbox performed seed-based analysis by calculating the temporal correlation between the average BOLD signals from a given seed to all other voxels in the brain. Fisher r to Z transformation was applied to correlation maps to achieve normality. Seeds-based functional connectivity was calculated for all subjects using a general linear model for Pearson's correlation coefficients estimation between the seed time course and the time course of all other voxels. Seeds-based functional connectivity was performed for all subjects using a weighted general linear model test to determine significant resting state seeds correlation at the individual level (1st level analysis). For each selected source seed, for each subject, first level results consisted in seed-to-voxel functional connectivity maps.

2nd level analysis. Following the computation of single subject connectivity maps, these maps were then entered into a second level general linear model to obtain population-level estimates. We used an uncorrected p-value height threshold of <0.001, with a cluster threshold of $p < 0.05$ (cluster-size p-FDR corrected) as the extent threshold for the whole brain. Finally, the significant differences in functional connectivity patterns between two different seeds was estimated by means of two paired t-tests for "between-source" differences (FWE p-FWE< 0.05 cluster-corrected, $p < 0.05$).

The 2nd level analysis was performed only on those sectors showing positive correlations. Since we performed paired t-tests to disclose only those areas showing higher connectivity, we excluded regions showing negative correlations to avoid the negative correlations in a contrast are significant. To this aim we used an explicit mask defined by those voxels that in the functional maps showed positive correlations.

2.9. Analysis of structural connections

In order to estimate the structural connectivity of investigated regions of interest we used an atlas of healthy white matter (Rojkova et al., 2016) part of the Tractotron tool in BCBToolkit software (http://toolkit.bcblab.com/; Foulon et al., 2018). The Recruitment and Suppression sectors of both hemispheres were extended in order to include the surrounding white matter until the fundus of the precentral sulcus. We overlaid the different functional sectors with likely white matter tracts that support hand motor function. These included the corticospinal tract

and fronto-striatal tracts, but also frontal aslant tract (Budisavljevic et al., 2017), superior longitudinal fasciculus I-III (Budisavljevic et al., 2017) and U-shaped precentral-postcentral tracts in the hand region (Catani et al., 2012; Thompson et al., 2017).

3. Results

3.1. Spatial localization of seed for rsfMRI

The probability density estimation was applied on the anatomical coordinates of each effective site. The surface volume obtained from each density estimation analysis was threshold in order to include only those volumes showing a probability greater than or equal to 35% (Fig. 1, for further details see Fornia et al., 2019). Four intraoperative seeds (left Recruitment sector, left Suppression sector, right Recruitment sector, right Suppression sector) in the precentral gyri of both hemispheres were identified based on the effect of DES delivered on the precentral gyrus in patients. These were then used to compute resting-state fMRI-derived functional connectivity in healthy brains. Seed volume did not differ significantly between seeds: left Recruitment sector (mean coordinates $x = -49 \pm 7sd$ $y = -4.7 \pm 3.7sd$ $z = 54.6 \pm 9.3sd$), $n = 124$ voxels; left Suppression sector (mean coordinates $x = -58.9 \pm 1.9sd$ $y = 3.2 \pm 3.6sd$ $z = 34.9 \pm 7.7sd$), $n = 130$ voxels; right Recruitment sector (mean coordinates $x = 38.6 \pm 2.3sd$ $y = -10.6 \pm 2.4sd$ $z = 68.4 \pm 1.9sd$), $n = 183$ voxels; right Suppression sector (mean coordinates $x = 55.8 \pm 10sd$ $y = 3.1 \pm 7sd$ $z = 38.2 \pm 16sd$), $n = 209$ voxels.

3.2. Spatial distribution of tumor

The spatial distribution of the tumors in the 66 patients is shown in Fig. 2. In the patients with the tumor located in the right hemisphere, the region of maximum overlap ($n = 5$ patients) was located anterior to the investigated area, while in the patients with tumors situated in the left hemisphere the maximum overlap was ventral to the right precentral gyrus. No patients used for analysis had any preoperative motor deficits. The right and left precentral gyri were not infiltrated by the tumor in any of the patients.

3.3. Functional connectivity of dorsal (recruitment) and ventral (suppression) sectors of the precentral gyrus involved in hand-object interaction

Intraoperative results were collected from a population of 66 tumor patients undergoing awake surgery for a brain tumour requiring the intraoperative mapping technique used to identify functional borders for resection implemented with the dedicated hand manipulation task. Two distinct regions within the precentral gyrus emerged to be related to control of hand-object interaction. The effect of DES on the regions identified in patients with a tumor located in the left hemisphere were described in a previous study of our group (Fornia et al., 2019). DES delivered on the dorsal PMv and ventro-caudal PMd of patients with a tumor located in the right hemisphere led to similar results (unpublished data). DES delivered over the precentral gyrus during hand-manipulation task execution disrupted the hand manipulation task (Fig. 1A). Two different effects of DES were observed from the EMG of hand muscles, a decrease (Suppression, Fig. 1B3) and increase (Recruitment, Fig. 1B2) in motor units involved in the task execution (for details see Fornia et al., 2019). Specifically, these distinct changes in muscle activity occurred in sites clustered within the ventral (Fig. 1C2, 1C4) and dorsal sector respectively (Fig. 1C1, 1C3). The Suppression and Recruitment recorded in this setting were then used as seeds to compute resting-state functional networks in healthy subjects provided by the WU-Minn Human Connectome Project (HCP) consortium (Van Essen et al., 2013). To avoid the neural changes of whole-brain functional connectivity associated with the tumor pathology itself, we computed this measure in an independent sample of healthy subjects.
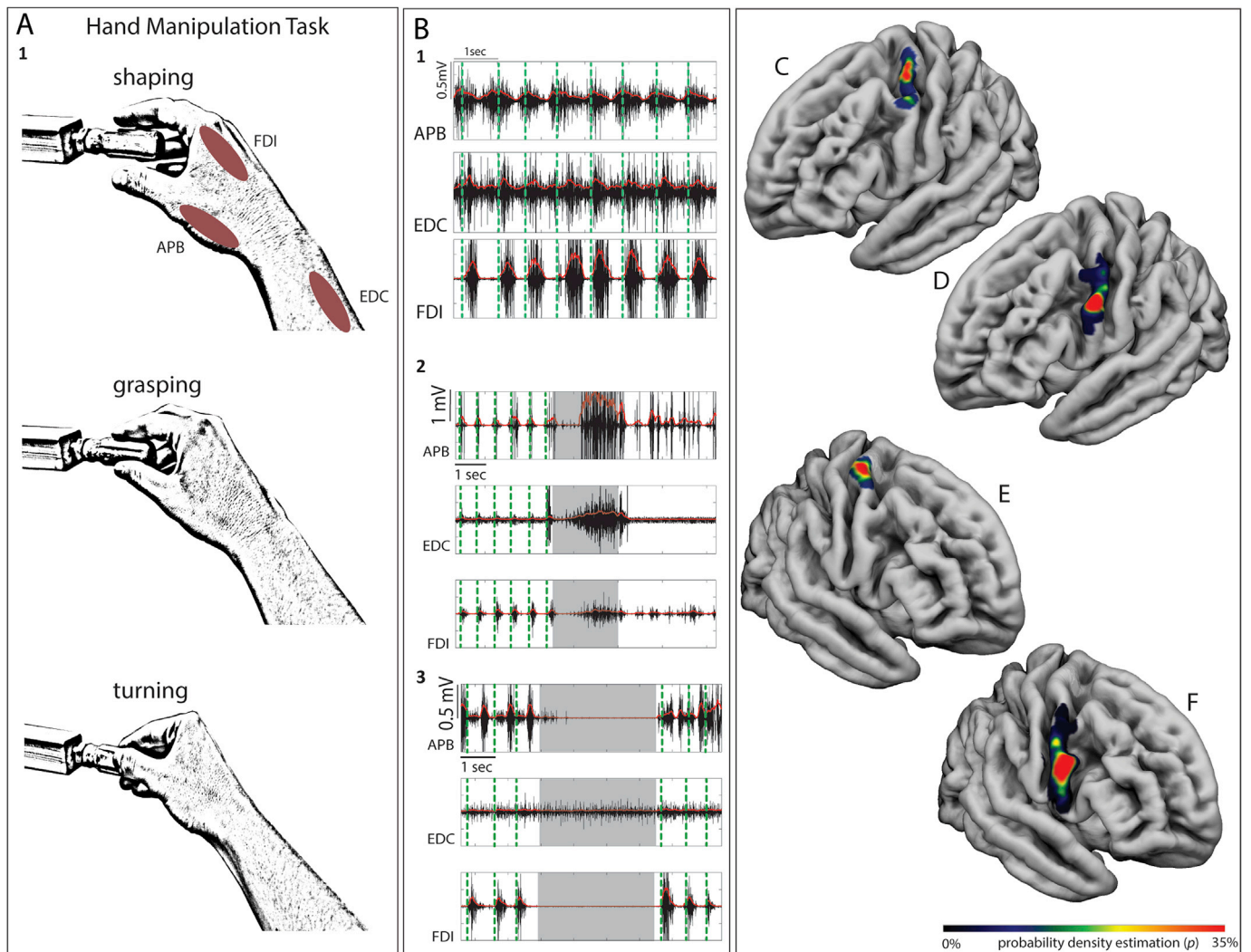
Fig. 1. A) Hand manipulation task. Schematic representation of the hand manipulation task execution and localization of the muscles recorded during its execution (APB, Abductor Pollicis Brevis; FDI, First Dorsal Interosseous; EDC, Extensor Digitorum Communis). B_1) Example of EMG activity from the muscles recorded during hand manipulation task execution without stimulation, B_2) Example of EMG activity during stimulation of the ventro-caudal PMd evoking a clear muscle recruitment preceded by brief Suppression immediately after DES onset. B_3) Example of EMG activity during stimulation of the dorsal PMv evoking a clear muscle Suppression. On the EMG activity of each muscle the vertical green dashed line indicates the time in which the patient approached the object (shaping). The time between green vertical dashed lines indicates the time required by each patient to shape the fingers immediately before the contact with the object, to grasp it, to rotate it and turning back to the initial shaping phase. C) localization of the RMS Recruitment and Suppression responses in the left hemisphere (respectively 1 and 2) and right hemisphere (respectively 3 and 4).

3.4. Functional connectivity of left and right recruitment sectors (recruitment) in dorsal PMv

We computed the functional connectivity of the premotor sector in each hemisphere where DES, delivered during hand manipulation task execution, increased recruitment of muscle activity (Recruitment). Fig. 3A and 3. B show the functional connectivity of the left and right Recruitment sectors respectively. It is noteworthy that left and right Recruitment sectors show very similar connectivity maps in both hemispheres. Resting-state fMRI-derived functional connectivity patterns of both sectors ($p < 0.05$, FWE-corrected at the cluster level) encompassed a bilateral set of areas including almost the entire dorsoventral extent of the primary sensory and the primary motor regions and the premotor areas of the caudalmost part of the superior, middle, and inferior frontal gyri. These networks also included a region corresponding to the supplementary motor area (SMA), extending medially into the anterior and posterior cingulate cortex and laterally to the central opercular cortex and the secondary somatosensory cortex, anterior supramarginal gyrus and superior parietal lobule. In the left hemisphere, a functional connection between a large portion of the posterior and middle insula (Fig. 3A left) and the lateral occipital complex (LOC) was evident. In summary, in both hemispheres the recruitment regions were functionally connected to a common network of fronto-parietal cortical regions, also including the LOC and insular components in the left hemisphere.

3.5. Functional connectivity of left and right suppression (suppression) sectors in ventro-caudal PMd

The same analysis was performed in both the left and right hemispheres for the Suppression sector, where DES delivered during the hand manipulation task resulted in transient suppression of the hand manipulation task. The networks emerging from the rsfMRI functional connectivity analysis of the Suppression sector ($p < 0.05$, FWE-corrected at the cluster level, Fig. 3C and Fig. 3D) were very similar to the network emerging from the Recruitment sector (Fig. 3A and Fig. 3B), especially in the parietal components, in both hemispheres. The key difference was
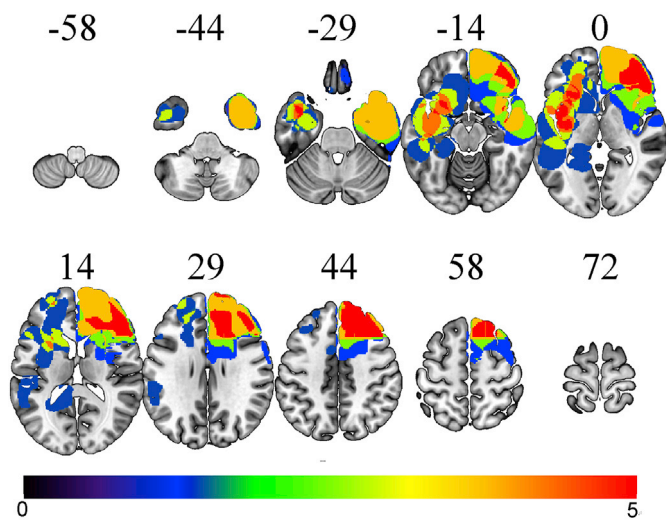
Fig. 2. Topography of lesions location of the patient with tumor localised in the left and right hemisphere. Left and right precentral gyri were not infiltrated by the lesion.

that, unlike the Recruitment sector, the Suppression sector was not functionally connected to the dorsalmost regions of primary motor and sensory areas, the caudal cingulate cortex, and the posterior part of the insula. Irrespective of the seed, there was also considerable functional connectivity between the four seeds.

3.6. Comparison of functional connectivity in ipsilateral intraoperative regions

To assess differences in functional coupling in the ipsilateral Recruitment and Suppression sectors two paired t-tests were performed. These tests were aimed at disclosing possible differences of functional connectivity of the Recruitment and Suppression sectors of the same hemisphere (i.e 4×2 paired *t*-test: left Recruitment > left Suppression and left Suppression > left Recruitment, right Recruitment > right Suppression and right Suppression > right Recruitment). The results showed that the left Recruitment sector, compared to the Suppression sector in the same hemisphere, showed stronger functional connectivity bilaterally with the cortical sector likely hosting the hand representation of precentral and postcentral gyri, the SMA, and middle frontal gyrus, superior parietal lobe and the insula of the left hemisphere (height threshold of <0.001 p uncorrected, cluster threshold $p < 0.05$ p-FWE cluster-corrected) (Fig. 4A). Similarly, in the right hemisphere, the Recruitment sector, displayed higher functional connectivity compared to the Suppression sector, centered on the hand representation of the precentral and postcentral gyri of the right hemisphere being localised in a region called the 'hand-knob' due to its visible omega in axial MR images (Fig. 4B). In the left hemisphere, functional connectivity of the Suppression sector was not stronger than the Recruitment sector. Interestingly, in the right hemisphere the right Suppression sector was stronger than the right Recruitment bilaterally in functional connectivity with the precentral gyri, SMA, superior frontal gyri, LOC, paracingulate gyri, middle temporal gyri and at supramarginal gyrus, superior parietal lobe, insula, parietal and frontal opercula (Fig. 4C, height threshold of <0.001 p uncorrected, cluster threshold $p < 0.05$ p-FWE corrected).
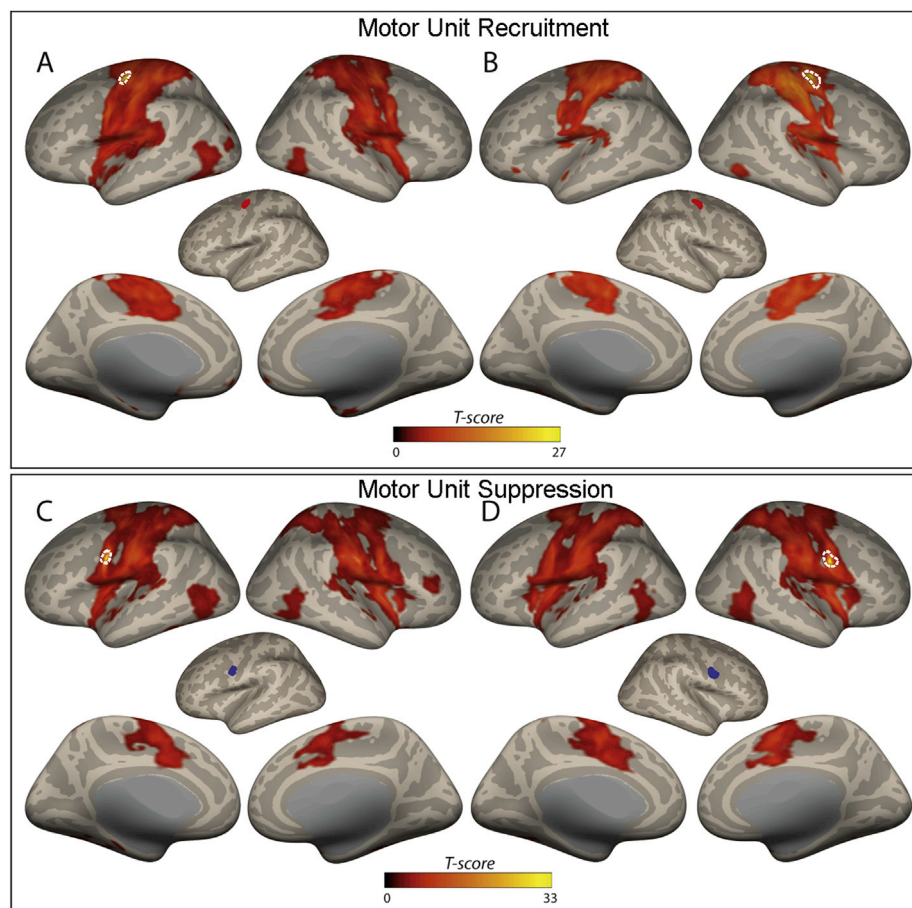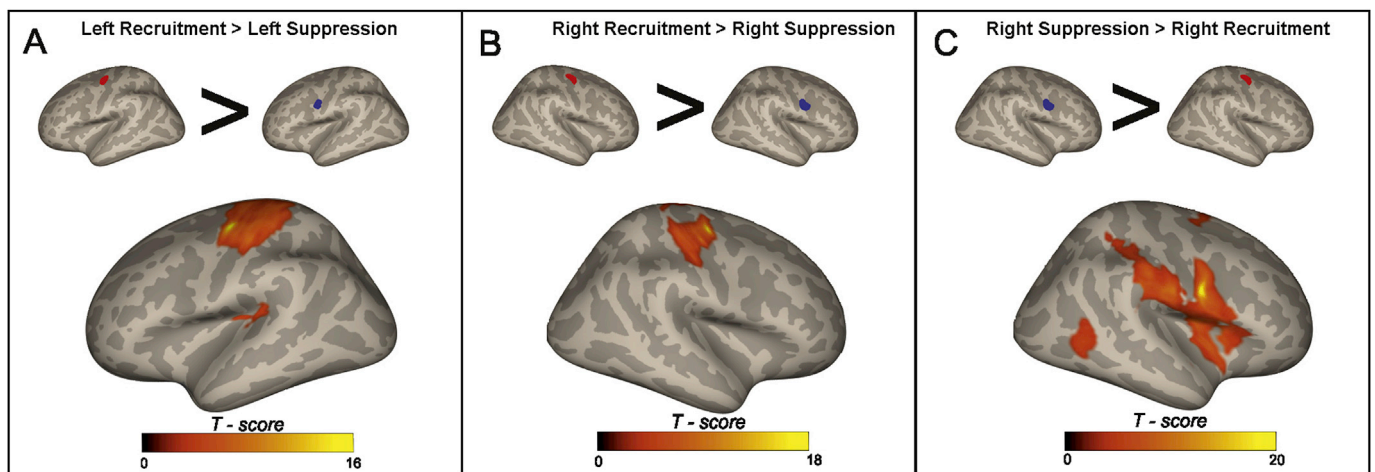

Fig. 3. Functional connectivity (FC) maps of the Recruitment (Red seeds) and Suppression sectors (Blue seeds). FC maps of the of Left (A) and Right (B) Recruitment and of the Left (C) and Right (D) Suppression. The dashed lines on the FC maps represent the borders of the seeds. $p < 0.05$, FWE-corrected at the cluster level.

Fig. 4. Comparison of FC of ipsilateral Recruitment (red) and Suppression (blue) sectors of the left and right hemisphere (Two paired t-tests height threshold of <0.001 p uncorrected, cluster threshold p < 0.05 p-FWE cluster-corrected). A: FC of the left Recruitment sector was stronger than that of left Suppression sector in the hand representation of the precentral and post central gyri of both hemispheres. B: FC of the Right Recruitment sector was stronger than that of the Right Suppression sector in the hand representation of the precentral and post central gyri of the right hemisphere. C: FC of the right Suppression sector was higher than that of the right Recruitment sector in a bilateral parieto-frontal network.

3.7. Comparison of the functional connectivity of DES -effective and DES-ineffective regions

Direct electrical stimulation of a cortical sector anatomically located between the Recruitment and Suppression sectors did not disrupt the hand manipulation task execution (DES-ineffective regions). In order to test whether the rsfMRI can detect differences in functional connectivity between effective and ineffective regions, we compared the seed-based correlations of Recruitment and Suppression with the seed-based correlations of the ineffective sector within the ipsilateral precentral gyrus (i.e two paired t-test: left and right Recruitment and Suppression seeds > left and right ineffective seeds). Fig. 5 shows the results of this analysis. Functional connectivity of the left Recruitment sector (Fig. 5) was stronger than the left ineffective area with the dorsal portion of the precentral and postcentral gyri bilaterally. Functional connectivity of the right and left Suppression sectors was not significantly stronger than the ipsilateral ineffective regions, except with regions in immediate proximity (intraregional connectivity). This was also the case for the right Recruitment sector. The results of this analysis show that among all the DES-effective sites (left and right Recruitment and left and right Suppression), only the left Recruitment showed stronger functional connectivity, compared to the ineffective sectors of the same hemisphere. Interestingly, the cortical sectors that were more strongly functionally connected with this sector were the ipsilateral and contralateral hand-related precentral and postcentral regions. These results indicate that although effective and ineffective regions underly similar functional networks, the left Recruitment sector was more strongly functionally connected bilaterally with the hand-field representation of the precentral and postcentral gyri, thus possibly reflecting the "effector-specificity" of this regionFig. 6.

3.8. Structural connections of recruitment and suppression sectors

Tractotron provided an indicator quantifying the degree of overlap between a chosen seed voxel and a voxel with high probability containing a specific white matter tract, based on an atlas of healthy white matter. We used a cut-off of 50% probability to identify the white matter tracts known to be involved in the sensorimotor control. As result the Recruitment sectors in both hemispheres overlapped with regions hosting the superior longitudinal fasciculus II (SLFII) (Fig. 6A) and the frontostriatal tract (FST) (Fig. 6C). The right Recruitment sector was also highly
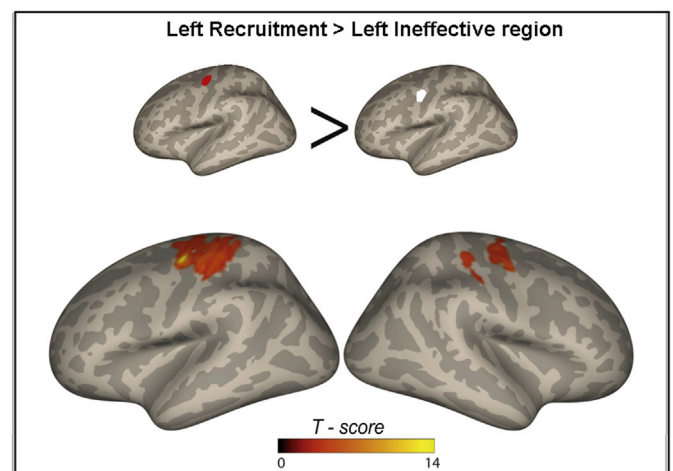

Fig. 5. Comparison of the functional connectivity of the intraoperative seeds with those of ineffective DES regions. (Two paired t-test: left and right intra seeds > left and right ineffective seeds). Only the FC of left Recruitment (red) was stronger with respect to that of the ineffective ipsilateral DES seed (white) in some cortical regions. All the other comparisons (not shown) yielded a stronger correlation of the effective seed with the cortex surrounding its location (intraregional connectivity).

overlapping with the hand U-shaped tracts connecting the precentral and postcentral gyrus. The Suppression sectors in both hemispheres intersected with the frontal aslant tract (FAT) (Fig. 6E) the hand inferior U-shaped tracts (Fig. 6F) and the SLFIII (Fig. 6D). Overall these results suggested that the two sectors were characterized by distinct short-frontal intralobar and parieto-frontal connections. In addition, the two sectors showed a different access to corticofugal pathway (CST), significantly prevalent in the recruitment sectors (Fig. 6B).

4. Discussion

Tool manipulation by the hands is a highly developed human ability that hugely facilitates all everyday life activities. The premotor cortex is a key component of the cortical network involved in controlling these skilled hand actions. Most knowledge about the role played by this frontal sector during the execution of goal-directed manipulative actions
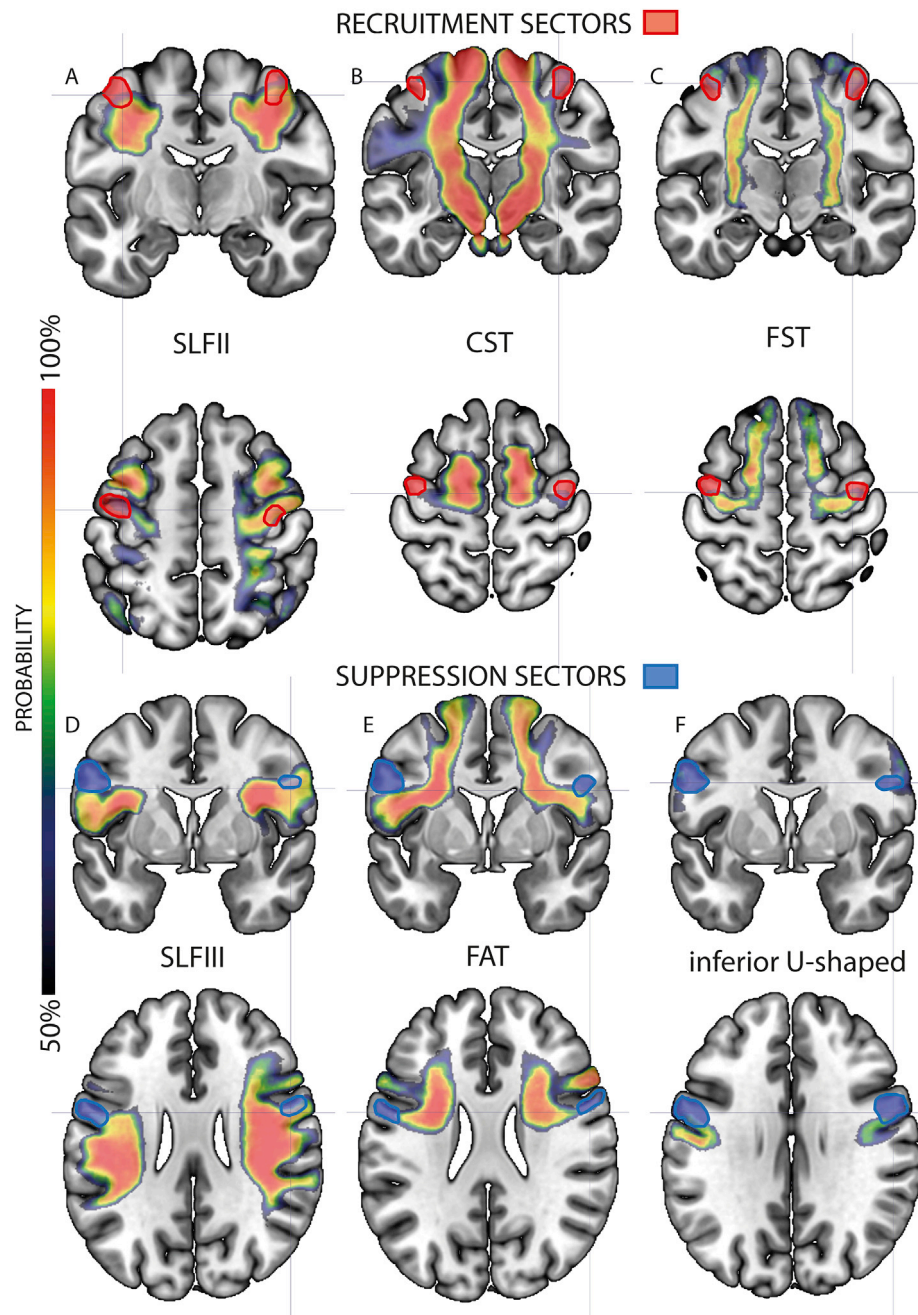
Fig. 6. The figure shows the main white matter tracts overlapping with the Recruitment (Red) and with the Suppression (Blue) sectors. A) Superior Longitudinal Fasciculus II, SLFII; B) CorticoSpinal Tract, CST; C) Fronto-Striatal Tract, FST; D) Superior Longitudinal Fasciculus III, SLFIII; E) Frontal Aslant Tract, FAT; F) Hand Inferior U-shaped fibers.

has been obtained through invasive experiments carried out on non-human primates (Rizzolatti et al., 1988). Results obtained from human functional imaging studies have proved that, akin to what has been observed in monkeys, the premotor cortex is involved in hand-object interaction, but there is little evidence on its possible functional organization in subserving this ability. A crucial aspect of imaging studies investigating the rsfMRI functional connectivity is the choice of cortical regions/seeds that are used as seeds for the analysis. Electrophysiological investigation on the macaque has allowed for the identification of sub-sectors of premotor cortex exerting different roles in control of hand movement (Bonini et al., 2012), thus the choice of seeds for the imaging analysis should be based on the same principle, and thus on functional rather than anatomical seeds. The brain mapping technique used for brain tumour removal facilitates direct access to brain structures and

provides data comparable, to some extent, to those obtained in non-human primate studies. Based on this premise, we investigated the functional connectivity of two regions of the precentral gyrus strictly related to hand-tool manipulation identified in the unique intraoperative setting during brain tumour resection. This setting enables the quantification of the effect of the direct electrical stimulation on different sectors of the cortex in awake patients performing a dedicated hand-manipulation task. The novelty of this study was that we did not use anatomical seeds defined using a standard brain atlas, rather we used two specific cortical sectors identified on the basis of the individual sites recorded where DES impaired the task during the operation of 36 patients in the left and 30 patients in the right hemisphere. By combining EMG and spatial analysis we demonstrated that these two sectors show different functional properties: the quantitative analysis of the activity

recorded from hand muscles during task performance during DES showed a Suppression sector inducing an inhibition of muscle recruitment and a Recruitment sector inducing a dysfunctional increase in muscle recruitment (Fornia et al., 2019). We identified the functional networks in a population of healthy subjects from the Human Connectome Project (Van Essen et al., 2013).

The main aim was to understand whether two sectors involved in control of a highly skilled hand movement may exert different roles reflected in different functional networks or rather if they share a common circuit with similar or preferential functional connections within the areas belonging to the network.

The networks emerging from the functional analysis of these two sectors in both hemispheres were similar and included mainly the precentral and postcentral gyri, the SMA, the secondary somatosensory area, the superior parietal cortex, the rostral inferior parietal cortex, the caudal and middle insula and the LOC. The difference in the pattern of functional connections of these two seeds was found in the relative extension of correlated cortical regions. Interestingly, the common pattern of functional connectivity shown by Recruitment and Suppression seeds overlapped with the functional network that is activated during hand motor tasks detected with fMRI. Specifically, execution of object-oriented hand actions activates frontal, parietal and insular regions largely corresponding with those functionally connected with the Recruitment and Suppression sectors as well as the LOC (Culham et al., 2003; Binkofski et al., 1999; Gallivan et al., 2013). This finding is supported by the evidence that functional coupling at rest is the result of the coactivation of regions embedded into the same functional network (Shulman et al., 1997; Corbetta and Shulman, 2002; Smith et al., 2009) and that patterns of coherence at rest may be promoted by coordinated neuronal activity among the areas that are actually involved in a given task. The main difference between the functional networks from hand task-fMRI and rsfMRI is that the task-fMRI may be more selective in activating more restricted regions of the precentral and postcentral gyri, involving mainly their hand representations, but fails to detect activation of other parietal and prefrontal areas. Biswal et al. (1995) computed the rsfMRI of seeds corresponding to the hand representation of the primary motor cortex identified using a finger tapping task and described a "sensorimotor network" including only the precentral and postcentral gyri and the SMA. A similar "sensorimotor network" was described by Yeo et al. (2011) using functional connectivity based on a cluster approach, but also in this case the functional network identified did not include the parietal or prefrontal cortex. Conversely, the functional network identified using all seeds (Suppression and Recruitment left and right) in the present study includes strong connections with association areas such as the inferior and superior parietal areas, as well as the posterior insula and LOC. This seems coherent with the evidence that, on one side, the LOC is known to play a role in object recognition and in coding perceptual information about objects, crucial to achieve an appropriate grasp (e.g., Grill-Spector et al., 2001; Verhagen et al., 2008) and on the other side, the mid-posterior insula is anatomically connected with the hand representation of the parietal and frontal regions controlling reaching/grasping actions in both monkeys (Jezzini et al., 2012) and in humans (Cerliani et al., 2012; Ghaziri et al.,2015; Di Cesare et al.,2018). Both these areas are indeed expected to be involved in a network subserving hand actions. The discrepancy between the previous studies and the present one might be explained by the location of the seeds used for rsfMRI analysis: our seeds were located on the convexity of the precentral gyrus, reasonably in the premotor cortex, and they have been functionally identified with a task requiring hand manipulation, while the seeds used in Biswal et al. (1995) and in Yeo et al. (2011) were located in the anterior bank of the central sulcus, reasonably in the hand representation of the primary motor cortex. Therefore, considering that functional connectivity should be constrained by structural connectivity, such differences could reflect differences in the anatomical networks underlying premotor and primary motor hand representations.

An important aspect deserving discussion is the difference between the functional connectivity of the two regions used as seeds for the analysis. Despite the very similar cortical functional networks shared by Recruitment and Suppression, the effect of their stimulation in motor output perturbation points to a different role of the two sites involved in control of the task (Fornia et al., 2019). This could be explained by a differential connectivity of these two areas exerted either by descending cortical projections or by cortico-cortical connections. Hand manipulation task disruption might indeed be due to the interruption of signal transmission through the corticospinal fibers from both Recruitment and Suppression sites. However, in this respect the contribution to the corticospinal system might be significantly more associated to the more dorsal region (see below), where relevant corticospinal outputs originate. hand manipulation task disruption might also be due to the interruption of signal transmission between the stimulated regions (both Suppression and Recruitment) and the cortical areas embedded in their functional network. The perturbation of any "hub" in a circuit is expected to impair the output of the circuit with different features depending on the role exerted by the hub. This effect was demonstrated in studies showing that electrical stimulation of lateral geniculate nucleus activates V1 while suppressing the activity in V2 and the extrastriate areas, disrupting cortico-cortical signal propagation by silencing the output of the stimulated areas (Logothetis et al., 2010). Considering the significant overlap between the networks emerging from the analysis based on the two different seeds (Recruitment and Suppression) it may not be possible to identify, with rs-fMRI the unique neural substrate responsible for the different effects of DES. However, when analysing the Recruitment and Suppression functional networks more closely, some differences emerged. Specifically, the Recruitment sector, compared to the Suppression sector was more strongly functionally connected with the upper limb representations of the precentral and postcentral gyri with a strong left dominance suggested by more widespread functional connectivity network of the left Recruitment with respect to the right one. These differences were confirmed by the results emerging from the comparison of the functional connectivity of Recruitment and Suppression seeds with those of the "ineffective" sectors. Indeed, only the left Recruitment sector had significantly higher functional connectivity with both banks of the ipsilateral central sulcus and the dorsal portion of the bilateral precentral and postcentral gyri, corresponding to hand representations (Culham et al., 2003). In summary, the analyses suggest that, despite widespread connections of the Recruitment sector with a broad region of the motor, premotor, and somatosensory cortex, it is clearly strongly and preferentially coupled (especially on the left) with hand representations, unlike adjacent "ineffective" and suppression cortical sites. This finding is coherent with recent studies based on diffusion weighted imaging (DWI) and rsfMRI, showing that PMd can be parcellated into five distinct subregions, the more caudal and motor-related sector (Genon et al., 2017) likely overlapping with the Recruitment sector of the present study. Altogether this data suggests that the left Recruitment has preferential and direct access with descending motor projections through M1, thus DES delivery on this sector, though not evoking responses at rest, could increase the excitability of the Recruitment sector-M1 connections, which are highly excitable during task execution (Bonini et al., 2012; van Wijk et al., 2012).

In the present study, the patients belonging to the population analysed to obtain the seeds were right handed. The central sulcus of the dominant hemisphere is deeper with respect the non-dominant one (Amunts et al., 1996) and handedness is associated with differences in the right and left hemispheres in white matter tracts connecting frontal premotor and parietal regions (Howells et al., 2018). It is well known that hand dominance influences extension of the activation of the contralateral primary motor hand representation (Dassonville et al., 1997; Volkmann et al., 1998) and the functional architecture of the motor system even at rest (Pool et al., 2015). Based on these premises it cannot be excluded that significant differences between the functional connectivity of the "ineffective sites", that emerge only when compared with the left Recruitment, may be due to higher BOLD correlation signals linked to the

handedness of the subjects.

Differently, the Suppression sector, located within the PMv, fails to show functional connections with the hand fields of the precentral and postcentral gyri in both hemispheres. Furthermore, the right Suppression sector showed stronger functional connectivity with respect to the right Recruitment sector in a bilateral set of parieto-frontal areas representing the core of a large-scale network that may be the possible substrate for integration of perceptual and cognitive with hand-related sensorimotor process for generating goal-related hand action (lateral grasping network, Borra et al., 2017). Therefore, the right Suppression sector, and its related functional network, could play a role in visuomotor transformations for grasping, in which visual coding of the object's properties automatically leads to the activation of distal movement representations appropriate for hand-object interactions (Jeannerod et al., 1995). This hypothesis is also supported by the stronger functional connection between Suppression and LOC region.

The parieto-frontal network was only identified from the right Suppression sector, and this asymmetry is likely the result of the Recruitment sector left dominance mentioned above, since the left Recruitment sector is among the intraoperative seeds showing higher functional connectivity, the left Suppression sector failed to show the parieto-frontal functional network highlighted in the right hemisphere. In a recent rsfMRI comparative study, the human PMv has been first subdivided into two regions based on DWI (Neubert et al., 2014), the more dorsal (6v) located in a cortical sector likely including the Suppression region. The functional connectivity pattern of 6v region resembles that of the Suppression sectors, as it does not include the dorsalmost regions of the primary sensory and primary motor area bilaterally, but, differently from Suppression, it lacks the LOC, suggesting that Suppression might be a functionally defined subsector of 6v region. Interestingly, PMv has also been subdivided into more than two regions according to cyto- and receptor-architectonic data (Amunts et al., 2010). DES delivered on the precentral gyrus in the PMv and the ventralmost part of PMd, showed three sectors characterized by different excitability thresholds and somatotopy, located at different dorsoventral levels (Fornia et al., 2018). The Suppression region is very likely located in correspondence of the middle one of these sectors, in which DES elicited oro-hand motor evoked potentials (MEP) at higher thresholds with respect to the more dorsal "hand" sector. Also in the non-human primate PMv there are sectors characterized by different excitability thresholds and somatotopy. Specifically, in the macaque, there is a more dorsal area (F5p) connected with the primary motor cortex, origin of corticospinal projections, where intracortical microstimulation (ICMS) is effective in evoking hand movements at relatively low thresholds and there are more ventral and rostral areas (F5a and F5c) where ICMS is not effective, neurons show hand and mouth motor properties (Maranesi et al., 2012) and visual properties are predominant (Schaffelhofer and Scherberger, 2016). It is possible that also in the human PMv there are various sectors differentially involved in motor and visuomotor processing for hand motor control. Based on the available data, it is not yet possible to establish clear correspondences.

Regarding the structural analysis our results highlighted that the Recruitment and Suppression sectors in both hemispheres were subserved by hand-related U-shaped fibers, that play a crucial role in hand motor control (Cerliani et al., 2012; Thompson et al., 2017). However, our results indicated that, in both hemispheres, the SLF II and fronto-striatal tracts were connected with the Recruitment sector and the frontal aslant tract was connected with the Suppression sector. Structural asymmetry of both the SLF II and frontal aslant tract has been associated with different kinematic properties of reaching and grasping (Budisavljevic et al., 2017), and our results indicate that these tracts may have different functional significance in supporting hand motor function. Interestingly, the Suppression sector, mainly in the left hemisphere, was connected with the parietal lobe via the SLF III. However functional connectivity measures are not directly correlated with anatomical connectivity (Honey et al., 2009), and our results may highlight that closer comparison of functional and anatomical connectivity in these regions is required.

5. Limitations

A limitation of our study is that the intraoperative seeds and the functional networks are derived from different individuals therefore we could not describe the functional network in the same brains where the intraoperative seeds were defined. However, two issues can moderate these limitations. First, within each hemisphere, Recruitment and Suppression seeds were defined within a large cohort of patients and, to compensate for sparse sampling, anatomical clustering of the seeds was estimated by means of a probability density function. Thus, the anatomical localization and the functional characterization of our seeds are the result of highly conserved cortical stimulation sites despite possible inter-individual variations in more widespread cortical architecture of cerebral functions that may have been induced by the glioma. Second, the intraoperative seeds were defined in patients in which a wide region of the precentral gyrus including the two seeds was not infiltrated by the tumor, therefore were less susceptible to be spatially reorganized.

6. Conclusion

Networks identified by resting state functional connectivity analysis (rsfMRI) are suggested to represent the fundamental units of brain organization, enrolled and integrated to perform tasks (Deco and Corbetta, 2011). In the present study we performed rsfMRI analysis in healthy subjects, using data obtained in patients in neurosurgical intraoperative setting to describe the functional connectivity of two specific brain regions located in the precentral gyrus (Recruitment and Suppression) involved in hand-object interaction. Intraoperative stimulation of these two sites impaired the execution of hand manipulation either by inducing a Suppression of the muscle activity (Suppression site) or by inducing dysfunctional hand muscle recruitment (Recruitment site). The functional connectivity pattern of these two intraoperative seeds is highly similar involving premotor and parietal and occipito-temporal regions active during hand motor task, but the emergence of different connections supports the idea of different roles exerted by the two sectors in controlling hand motor behavior. However, despite widespread functional connections of Recruitment sector with parieto-frontal regions, it is strongly coupled with the cortical sector likely hosting the hand representations in sensorimotor cortex, suggesting its role may be linked to corticospinal tract. Differently, the Suppression sector, showed stronger functional connectivity in a bilateral set of parieto-frontal areas involved in integration of perceptual and cognitive with hand-related action, thus stimulation of Suppression might halt high order sensorimotor integration processes needed to compute the motor output rather than acting on the motor output itself.

As translational impact, the combination of functional connectivity with intraoperative identification of the cortical sectors involved in muscle recruitment, might be a useful tool to precisely identify target brain regions of interventions (tDCS treatments etc) and to design specific rehabilitation protocols for recovery of motor function. Future experiments aimed at studying the activity of these seeds during different hand actions are mandatory to define their synergic role in shaping the hand motor behavior.

Conflicts of interest

The authors declare no competing financial interests.

Funding

Acknowledgements

Appendix A. Supplementary data

Supplementary data to this article can be found online at https://doi.org/10.1016/j.neuroimage.2019.116215.

References

Amunts, K., Schlaug, G., Schleicher, A., Steinmetz, H., Dabringhaus, A., Roland, P.E., Zilles, K., 1996. Asymmetry in the human motor cortex and handedness. Neuroimage 4, 216–222. http://DOI:10.1006/nimg.1996.0073.

Amunts, K., Lenzen, M., Friederici, A.D., Schleicher, A., Morosan, P., Palomero-Gallagher, N., Zilles, K., 2010. Broca's region: novel organizational principles and multiple receptor mapping. PLoS Biol. 21 (9), e1000489, 8. http://doi:10.1371/journal.pbio.1000489.

Baldassarre, A., Ramsey, L.E., Siegel, J.S., Shulman, G.L., Corbetta, M., 2016. Brain connectivity and neurological disorders after stroke. Curr. Opin. Neurol. 29 (6), 706–713 submitted for publication. http://DOI:10.1097/WCO.0000000000000396.

Behrens, T.E., Sporns, O., 2012. Human connectomics. Curr. Opin. Neurobiol. 22 (1), 144–153. http://doi:10.1016/j.conb.2011.08.005.

Bello, L., Riva, M., Fava, E., Ferpozzi, V., Castellano, A., Raneri, F., Pessina, F., Bizzi, A., Falini, A., Cerri, G., 2014. Tailoring neurophysiological strategies with clinical context enhances resection and safety and expands indications in gliomas involving motor pathways. Neuro Oncol. 16 (8), 1110–1128. http://doi:10.1016/j.conb.2011.08.005.

Binkofski, F., Buccino, G., Stephan, K.M., Rizzolatti, G., Seitz, R.J., Freund, H.J., 1999. A parieto-premotor network for object manipulation: evidence from neuroimaging. Exp. Brain Res. 128, 210–213. http://doi:10.1007/s002210050838.

Biswal, B., Yetkin, F.Z., Haughton, V.M., Hyde, J.S., 1995. Functional connectivity in the motor cortex of resting human brain using echo-planar MRI. Magn. Reson. Med. 34 (4), 537–541. https://doi.org/10.1002/mrm.1910340409.

Bonini, L., Ugolotti Serventi, F., Bruni, S., Maranesi, M., Bimbi, M., Simone, L., Rozzi, S., Ferrari, P.F., Fogassi, L., 2012. Selectivity for grip type and action goal in macaque inferior parietal and ventral premotor grasping neurons. J. Neurophysiol. 108, 1607–1619. https://doi.org/10.1152/jn.01158.2011.

Borra, E., Gerbella, M., Rozzi, S., Luppino, G., 2017. The macaque lateral grasping network: a neural substrate for generating purposeful hand actions. Neurosci. Biobehav. Rev. 75, 65–90. http://doi:10.1016/j.conb.2011.08.005.

Budisavljevic, S., Dell'Acqua, F., Djordjilovic, V., Miotto, D., Motta, R., Castiello, U., 2017. The role of the frontal aslant tract and premotor connections in visually guided hand movements. Neuroimage 1, 419–428. https://doi.org/10.1016/j.neuroimage.2016.10.051, 146.

Catani, M., Dell'Acqua, F., Vergani, F., Farah, M., Harry, H., Prasun, R., Romain, V., Michel, T. de S., 2012. Short frontal lobe connections of the human brain. Cortex 48 (2), 273–291. https://doi.org/10.1016/j.cortex.2011.12.001.

Cerliani, L., Thomas, R.M., Jbabdi, S., Siero, J.C.W., Nanetti, L., Crippa, A., Gazzola, V., D'Arceuil, H., Keysers, C., 2012. Probabilistic tractography recovers a rostrocaudal trajectory of connectivity variability in the human insular cortex. Hum. Brain Mapp. 33, 2005–2034. http://doi:10.1002/hbm.21338.

Corbetta, M., Shulman, G.L., 2002. Control of goal-directed and stimulus-driven attention in the brain. Nat. Rev. Neurosci. 3 (3), 201–215, 2002 Mar. http://DOI:10.1038/nrn755.

Culham, J.C., Danckert, S.L., DeSouza, J.F.X., Gati, J.S., Menon, R.S., Goodale, M.A., 2003. Visually guided grasping produces fMRI activation in dorsal but not ventral stream brain areas. Exp. Brain Res. 153, 180–189. https://doi.org/10.1007/s00221-003-1591-5.

Dassonville, P., Zhu, X.H., Uurbil, K., Kim, S.G., Ashe, J., 1997. Functional activation in motor cortex reflects the direction and the degree of handedness. Proc. Natl. Acad. Sci. U.S.A. 94 (25), 14015–14018. http://DOI:10.1073/pnas.94.25.14015.

Davare, M., Andres, M., Cosnard, G., Thonnard, J.L., Olivier, E., 2006. Dissociating the role of ventral and dorsal premotor cortex in precision grasping. J. Neurosci. 26 (8), 2260–2268. http://DOI:10.1523/JNEUROSCI.3386-05.

Davare, M., Lemon, R., Olivier, E., 2008. Selective modulation of interactions between ventral premotor cortex and primary motor cortex during precision grasping in humans. J. Physiol. 586 (11), 2735–2742. http://DOI:10.1113/jphysiol.2008.152603.

Davare, M., Montague, K., Olivier, E., Rothwell, J.C., Lemon, R.N., 2009. Ventral premotor to primary motor cortical interactions during object-driven grasp in humans. Cortex 45 (9), 1050–1057. http://doi:10.1016/j.cortex.2009.02.011.

Deco, G., Corbetta, M., 2011. The dynamical balance of the brain at rest. The Neuroscientist 17 (1), 107–123. http://doi:10.1177/1073858409354384. Epub 2010 Dec 31. Review.

Di Cesare, G., Pinardi, C., Carapelli, C., Caruana, F., Marchi, M., Gerbella, M., Rizzolatti, G., 2018. Insula connections with the parieto-frontal circuit for generating arm actions in humans and macaque monkeys. 2018. Cerebr. Cortex bhy095. https://doi.org/10.1093/cercor/bhy095.

Dum, R.P., Strick, P.L., 2005. Frontal lobe inputs to the digit representations of the motor areas on the lateral surface of the hemisphere. J. Neurosci. 9 (25), 1375–1386, 6. http://DOI:10.1523/JNEUROSCI.3902-04.2005.

Ehrsson, H.H., Fagergren, A., Jonsson, T., Westling, G., Johansson, R.S., Forssberg, H., 2000. Cortical activity in precision- versus power-grip tasks. An fMRI Study 83 (1), 528–536. http://DOI:10.1152/jn.2000.83.1.528.

Fornia, L., Ferpozzi, V., Montagna, M., Rossi, M., Riva, M., Pessina, F., Martinelli Boneschi, F., Borroni, P., Lemon, R.N., Bello, L., Cerri, G., 2018. Functional characterization of the left ventrolateral premotor cortex in humans: a direct electrophysiological approach *Cerebr*. Cortex 28 (1), 167–183, 1. http://doi:10.1093/cercor/bhw365.

Fornia, L., Rossi, M., Rabuffetti, M., Leonetti, A., Puglisi, G., Viganò, L., Simone, L., Howells, H., Bellacicca, A., Bello, L., Cerri, G., 2019. Direct Electrical Stimulation of premotor areas shows different effects on hand-muscles activity during object manipulation. Cerebr. Cortex. https://doi.org/10.1093/cercor/bhz139.

Foulon, C., Cerliani, L., Kinkingnéhun, S., Levy, R., Rosso, C., Urbanski, M., Volle, E., Thiebaut de Schotten, M., 2018. Advanced lesion symptom mapping analyses and implementation as BCBtoolkit. GigaScience 7 (3), 1–17. https://doi.org/10.1093/gigascience/giy004.

Friston, K.J., Holmes, A.P., Poline, J.B., Grasby, P.J., Williams, S.C., Frackowiak, R.S., Turner, R., 1995. Analysis of fMRI time-series revisited. Neuroimage 2, 45–53. https://doi.org/10.1006/nimg.1995.1007.

Gallivan, J.P., McLean, D.A., Flanagan, J.R., Culham, J.C., 2013. Where one hand meets the other: limb-specific and action-dependent movement plans decoded from preparatory signals in single human frontoparietal brain areas. J. Neurosci. 30 (5), 1991–2008, 33. http://DOI:10.1523/JNEUROSCI.0541-12.2013.

Genon, S., Li, H., Fan, L., Müller, V.I., Cieslik, E.C., Hoffstaedter, F., Reid, A.T., Langner, R., Grefkes, C., Fox, P.T., Moebus, S., Caspers, S., Amunts, K., Jiang, T., Eickhoff, S.B., 2017. The right dorsal premotor mosaic: organization, functions, and connectivity. Cerebr. Cortex 27 (3), 2095–2110. https://doi.org/10.1093/cercor/bhw065, 1.

Ghaziri, J., Tucholka, A., Girard, G., Houde, J.-C., Boucher, O., Gilbert, G., Descoteaux, M., Lippé, S., Rainville, P., Nguyen, D.K., 2015. The corticocortical structural connectivity of the human insula. Cerebr. Cortex. http://DOI:10.1093/cercor/bhv308.

Glasser, M.F., Sotiropoulos, S.N., Wilson, J.A., Coalson, T.S., Fischl, B., Andersson, J.L., Xu, J., Jbabdi, S., Webster, M., Polimeni, J.R., Van Essen, D.C., Jenkinson, M., WU–Minn HCP Consortium, 2013. The minimal preprocessing pipelines for the Human Connectome Project. Neuroimage 80, 105–124. https://doi.org/10.1016/j.neuroimage.2013.04.127.

Grill-Spector, K., Kourtzi, Z., Kanwisher, N., 2001. The lateral occipital complex and its role in object recognition. Vis. Res. 41 (10–11), 1409–1422 submitted for publication. https://doi.org/10.1016/S0042-6989(01)00073-6.

Guerra-Carrillo, B., Mackey, A.P., Bunge, S.A., 2014. Resting-state fMRI: a window into human brain plasticity. Neuroscientist 20 (5), 522–533. https://doi.org/10.1177/1073858414524442. Review. Oct.

Honey, C.J., Sporns, O., Cammoun, L., Gigandet, X., Thiran, J.P., Meuli, R., Hagmann, P., 2009. Predicting human resting-state functional connectivity from structural connectivity. Proc. Natl. Acad. Sci. U. S. A. 106 (6), 2035–2040. https://doi.org/10.1073/pnas.0811168106, 10.

Howells, H., Thiebaut de Schotten, M., Dell'Acqua, F., Beyh, A., Zappalà, G., Leslie, A., Simmons, A., Murphy, D., Catani, M., 2018. Frontoparietal Tracts Linked to Lateralized HandPreference and Manual Specialization. Cerebr. Cortex. https://doi.org/10.1093/cercor/bhy040.

Jeannerod, M., Arbib A., M., Rizzolatti, G., Sakata, H., 1995. Grasping objects: the cortical mechanisms of visuomotor transformation. Trends Neurosci. 18, 314–320.

Jezzini, A., Caruana, F., Stoianov, I., Gallese, V., Rizzolatti, G., 2012. Functional organization of the insula and inner perisylvian regions. Proc. Natl. Acad. Sci. U. S. A. 19 (25), 10077–10082. https://doi.org/10.1073/pnas.1200143109, 109.

Logothetis, N.K., Augath, M., Murayama, Y., Rauch, A., Sultan, F., Goense, J., Oeltermann, A., Merkle, H., 2010. The effects of electrical microstimulation on cortical signal propagation. Nat. Neurosci. 13 (10), 1283–1291. https://doi.org/10.1038/nn.2631.

Maranesi, M., Roda, F., Bonini, L., Rozzi, S., Ferrari, P.F., Fogassi, L., Coude, G., 2012. Anatomo-functional organization of the ventral primary motor and premotor cortex in the macaque monkey. Eur. J. Neurosci. 36, 3376–3387. http://doi:10.1111/j.1460-9568.2012.08252.x.

Neubert, F.X., Mars, R.B., Thomas, A.G., Sallet, J., Rushworth, M.F., 2014. Comparison of human ventral frontal cortex areas for cognitive control and language with areas in monkey frontal cortex. Neuron 5 (3), 700–713. https://doi.org/10.1016/j.neuron.2013.11.012, 81.

Pool, E.M., Rehme, A.K., Eickhoff, S.B., Fink, G.R., Grefkes, C., 2015. Functional resting-state connectivity of the human motor network: differences between right- and left-handers. Neuroimage 1, 298–306. https://doi.org/10.1016/j.neuroimage.2015.01.034, 109.

Power, J.D., Cohen, A.L., Nelson, S.M., Wig, G.S., Barnes, K.A., Church, J.A., Vogel, A.C., Laumann, T.O., Miezin, F.M., Schlaggar, B.L., Petersen, S.E., 2011. Functional network organization of the human brain. Neuron 72, 665–678. https://doi.org/10.1016/j.neuron.2011.09.006.

Puglisi, G., Sciortino, T., Rossi, M., Leonetti, A., Fornia, L., Conti Nibali, M., Casarotti, A., Pessina, F., Riva, M., Cerri, G., Bello, L., 2018. Preserving executive functions in non-

dominant frontal lobe glioma surgery: an intraoperative tool. J. Neurosurg. 28, 1–7. https://doi.org/10.3171/2018.4.JNS18393.

Puglisi, G., Howells, H., Sciortino, T., Leonetti, A., Rossi, M., Conti Nibali, M., Gay, L.G., Fornia, L., Bellacicca, A., Viganò, L., Simone, L., Catani, M., Cerri, G., Bello, L., 2019. Frontal pathways in cognitive control: evidence from intraoperative stimulation and tractography. Brain 142, 2451–2465. http://doi:10.1093/brain.awz178.

Rizzolatti, G., Camarda, R., Fogassi, L., Gentilucci, M., Luppino, G., Matelli, M., 1988. Functional organization of inferior area 6 in the macaque monkey: II. Area F5and the control of distal movements. Exp. Brain Res. 71, 491–507. http://doi:10.17712/nsj.2 016.2.20150472.

Rojkova, K., Volle, E., Urbanski, M., Humbert, F., Dell'Acqua, F., Thiebaut de Schotten, M., 2016. Atlasing the frontal lobe connections and their variability due to age and education: a spherical deconvolution tractography study. Brain Struct. Funct. 221 (3), 1751–1766. http://doi:10.1007/s00429-015-1001-3.

Rossi, M., Fornia, L., Puglisi, G., Leonetti, A., Zuccon, G., Fava, E., Milani, D., Casarotti, A., Riva, M., Pessina, F., Cerri, G., Bello, L., 2018. Assessment of the praxis circuit in glioma surgery to reduce the incidence of postoperative and long-term apraxia: a new intraoperative test. J. Neurosurg. 23, 1–11. http://doi:10.3171/2017.7.JNS17357.

Schaffelhofer, S., Scherberger, H., 2016. Object vision to hand action in macaque parietal, premotor, and motor cortices. Elife 5. https://doi.org/10.7554/elife.15278.

Schreiber, A., Hubbe, U., Ziyeh, S., Hennig, J., 2000. The influence of gliomas and nonglial space-occupying lesions on blood-oxygen-level-dependent contrast enhancement. Am. J. Neuroradiol. 21 (6), 1055–1063.

Shulman, G., Corbetta, M., Buckner, R., Raichle, M., Fiez, J., Miezin, F., Petersen, S.E., 1997. Top-down modulation of early sensory cortex. Cerebr. Cortex 7, 193–206. https://doi.org/10.1093/cercor/7.3.193.

Smith, S.M., Fox, P.T., Miller, K.L., Glahn, D.C., Fox, P.M., Mackay, C.E., Filippini, N., Watkins, K.E., Toro, R., Laird, A.R., Beckmann, C.F., 2009. Correspondence of the brain's functional architecture during activation and rest. Proc. Natl. Acad. Sci. U. S. A. 4 (31), 13040–13045, 106. http://doi:10.1073/pnas.0905267106.

Smith, S.M., Beckmann, C.F., Andersson, J., Auerbach, E.J., Bijsterbosch, J., Douaud, G., Duff, E., Feinberg, D.A., Griffanti, L., Harms, M.P., Kelly, M., Laumann, T., Miller, K.L., Moeller, S., Petersen, S., Power, J., Salimi-Khorshidi, G., Snyder, A.Z., Vu, A.T., Woolrich, M.W., Xu, J., Yacoub, E., Uğurbil, K., Van Essen, D.C., Glasser, M.F., WU-Minn HCP Consortium WU–Minn HCP Consortium, 2013. Resting-state fMRI in the human connectome Project. Neuroimage 80, 144–168. http://doi:10.1073/pnas.0905267106.

Spinnler, H., Tognoni, G., 1987. Italian standardization of neuropsychological tests. Ital. J. Neurol. Sci. Suppl. 8, 1–120, 1987 (Italian).

Thompson, A., Murphy, D., Dell'Acqua, F., Ecker, C., McAlonan, G., Howells, H., Baron-Cohen, S., Lai, M.C., Lombardo, M.V., Catani, M., 2017. Impaired communication between the motor and somatosensory homunculus is associated with poor man-ual dexterity in autism spectrum disorder. Biol. Psychiatry 81, 211–219. https://doi.org/10.1016/j.biopsych.2016.06.020.

Ugurbil, K., Xu, J., Auerbach, E.J., Moeller, S., Vu, A.T., Duarte-Carvajalino, J.M., Lenglet, C., Wu, X., Schmitter, S., Van de Moortele, P.F., Strupp, J., Sapiro, G., De Martino, F., Wang, D., Harel, N., Garwood, M., Chen, L., Feinberg, D.A., Smith, S.M., Miller, K.L., Sotiropoulos, S.N., Jbabdi, S., Andersson, J.L., Behrens, T.E., Glasser, M.F., Van Essen, D.C., Yacoub, E., WU-Minn, HCP Consortium, 2013. Pushing spatial and temporal resolution for functional and diffusion MRI in the Human Connectome Project. Neuroimage 80, 80–104. http://DOI:10.1016/j.neu roimage.2013.05.012.

Van Essen, D.C., Smith, S.M., Barch, D.M., Behrens, T.E., Yacoub, E., Ugurbil, K., WU-Minn HCP Consortium, 2013. The Wu-minn human connectome Project: an overview. Neuroimage 80, 62–79. https://doi.org/10.1016/j.neuroimage.2013.05.0 41.

van Wijk C., B., Beek J., P., Daffertshofer, A., 2012. Neural synchrony within the motor system: what have we learned so far? Frontiers in human neuroscience 6, 1–12. https://doi.org/10.3389/fnhum.2012.00252.

Verhagen, L., Dijkerman, H.C., Grol, M.J., Toni, I., 2008. Perceptuo-motor Interactions during prehension movements. J. Neurosci. 28, 4726–4735. https://doi.org/10.15 23/JNEUROSCI.0057-08.2008.

Viganò, L., Fornia, L., Rossi, M., Howells, H., Leonetti, A., Puglisi, G., Conti Nibali, M., Bellacicca, A., Grimaldi, M., Bello, L., Cerri, G., 2019. Anatomo-functional characterization of the human hand-knob: a direct electrophysiological study. Cortex 113, 239–254. https://doi.org/10.1016/j.cortex.2018.12.011.

Volkmann, J., Schnitzler, A., Witte, O.W., Freund, H., 1998. Handedness and asymmetry of hand representation in human motor cortex. J. Neurophysiol. 79 (4), 2149–2154. http://DOI:10.1152/jn.1998.79.4.2149.

Wang, Z., Chen, L.M., Négyessy, L., Friedman, R.M., Mishra, A., Gore, J.C., Roe, A.W., 2013. The relationship of anatomical and functional connectivity to resting-state connectivity in primate somatosensory cortex. Neuron 19 (6), 1116–1126, 78. http://doi:10.1016/j.neuron.2013.04.023.

Yeo, B.T., Krienen, F.M., Sepulcre, J., Sabuncu, M.R., Lashkari, D., Hollinshead, M., Roffman, J.L., Smoller, J.W., Zöllei, L., Polimeni, J.R., Fischl, B., Liu, H., Buckner, R.L., 2011. The organization of the human cerebral cortex estimated by intrinsic functional connectivity. J. Neurophysiol. 106 (3), 1125–1165. https://doi.org/10.1152/jn.00338.2011.

Yordanova, Y.N., Cochereau, J., Duffau, H., Herbet, G., 2018. Combining resting state functional MRI with intraoperative cortical stimulation to map the mentalizing network. Neuroimage 1, 628–636. https://doi.org/10.1016/j.neuroimage.2018.11.046, 186.

Zacà, D., Corsini, F., Rozzanigo, U., Dallabona, M., Avesani, P., Annicchiarico, L., Zigiotto, L., Faraca, G., Chioffi, F., Jovicich, J., Sarubbo, S., 2018. Whole-brain network connectivity underlying the human speech articulation as emerged integrating direct electric stimulation, resting state fMRI and tractography. Front. Hum. Neurosci. 11 (12), 405. https://doi.org/10.3389/fnhum.2018.00405.